11527

Industrial Buildings with High Thermal Loads: Simulation of Natural Ventilation

Dieter Breer, Viktor Dorer

EMPA Swiss Federal Laboratories for Material Testing and Research, Section Building Equipment, CH-8600 Duebendorf Switzerland

ABSTRACT

In office and industrial buildings, the replacement of mechanical ventilation systems by natural ventilation systems is one suitable possibility to reduce the electrical energy consumption.

The modeling and simulation of thermally induced natural ventilation are presented here based on the example of a industrial laundry. An industrial laundry is a typical building with high internal thermal loads. For a representative summer case the outdoor air exchange and the room air temperatures in various zones were determined. The temperature evolutions were the result of simulations made with the computer program TRNSYS.

The openings for natural ventilation are often equipped with insect screens, which have an influence on the discharge coefficient C_d and thus on the flow resistance. This influence must be considered in the simulation and planning of the building and for this reason, different insect screens were measured in the air flow chamber at the EMPA. Both the grid distance and the opening cross-section were varied. The results show that insect screens have less influence on the discharge coefficient than expected. The simulations and the measurements indicate that with the planned openings high enough outdoor airflow rates result for the zones.

KEYWORDS

Simulation, Natural ventilation, Industrial buildings, Modeling

INTRODUCTION

During the past 25 years, the world energy demand of primary energy has been nearly doubled; the electrical energy demand during the same period has been tripled. Thus the need for the reduction of energy consumption, especially electrical, is very high. In office and industrial buildings, the replacement of mechanical ventilation systems by natural ventilation systems is one suitable option.

Comprehensive treatment of building ventilation can be found in (Etheridge et al., 1996), in (Awbi, 1991) and in (AIVC, 1996). Several researchers have studied the use of natural ventilation for cooling. A good summary on passive cooling can be found in (Santamouris et al., 1996). Little research has been done on simulation of naturally ventilated buildings with high thermal loads. The VDI-Guideline (VDI, 1997) gives suggestions for the use and the planning of ventilation systems in buildings with high thermal loads. Few additional suggestions could be found in the Clima Suisse documentation about the planning of ventilation systems for large rooms (Clima Suisse 1997).

The aim of the present paper is to describe, how natural ventilation can be used and simulated in industrial buildings with high thermal loads. The results of these studies could be useful for engineers responsible for the planning of such buildings. Conclusions are drawn concerning the possibilities and the limits of thermal simulation of naturally ventilated buildings.

SIMULATION OF NATURAL VENTILATION FOR A INDUSTRIAL LAUNDRY

Method

The behavior of a naturally ventilated industrial laundry with high thermal loads was simulated using computer tools

Building description

The examined building is a large industrial laundry, which cleans among other things hospital textiles; thus the requirements in respect with hygienic standards are high and the openings for the natural ventilation must be equipped with insect screens.

Internal thermal loads

Since the precise thermal loads were unknown at the time of the simulation, three different cases for the internal thermals loads were assumed (60/100/160 W/m²).

Simulation tools

For the calculations several software tools were used. The natural ventilation and the thermal behavior were computed with the dynamic building and system simulation program TRNSYS. In TRNSYS, the natural air flows were modeled as power law functions, basically considering stack effects. These functions were established using the COMIS model. The soil temperature distribution under the hall was determined with the finite element program FEET.

Space load factor

Outside air entering the space through openings near the ground spreads over the floor and absorbs energy from the floor surface. The resulting air temperature increase leads to buoyancy and forces the air up into the upper hall zone. This results in a temperature stratification in the hall. Due to this vertical temperature gradient, the air in

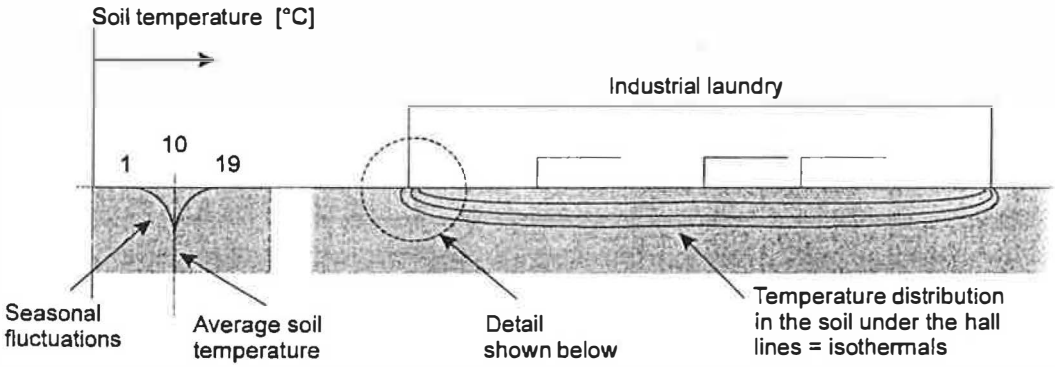

Figure 1 Representation of the temperature distribution in the soil under the laundry

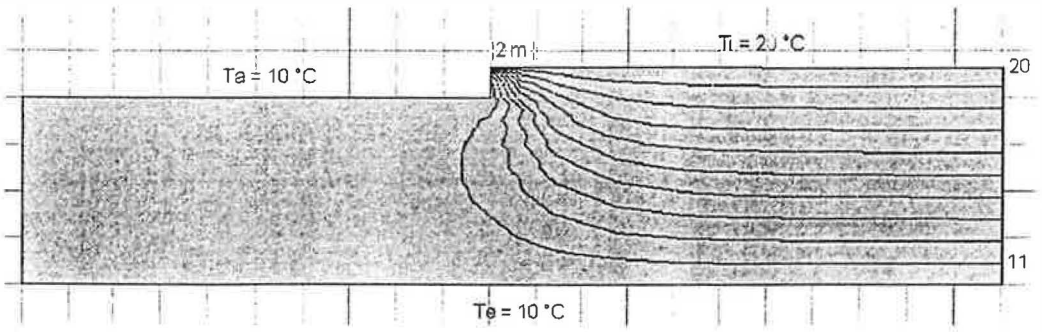

Figure 2 Result of the finite element calculation of the temperature distribution in the soil. The average soil temperature is 10°C.

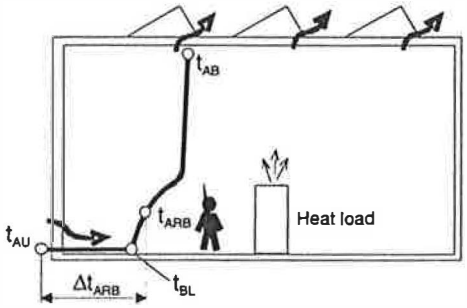

Figure 3 Temperature gradient related to the room height (schematic)

the occupied zone does not reach the exhaust air temperature t_{AB} (see figure 3). This has a positive effect on thermal comfort, particularly in the summer period.

The thermal space load factor is used to quantitatively characterize this effect:

$$\mu_t = \frac{t_{ARB} - t_{AU}}{t_{AB} - t_{AU}} = \frac{\Delta t_{ARB}}{t_{AB} - t_{AU}} \qquad (1)$$

The energy exhausted from the hall is:

$$\dot{Q} = \dot{m}_L \cdot c_p \cdot \frac{1}{\mu_t}\left(t_{ARB} - t_{AU}\right) \qquad (2)$$

The smaller the thermal load factor the more energy can be exhausted from the hall (with constant air temperature in the occupied zone).

Replacing the supply air mass flow $\dot{m}_L$ by the outside air change in equation (2) leads to :

$$\Delta t_{ARB} = \frac{\dot{q}_{To\ell} \cdot 3600}{n \cdot h \cdot \rho \cdot c} \cdot \mu_t \cdot \mu_g \qquad (3).$$

The term μ_g in equation (3) describes the thermal mass characteristic of the building for a day period. With thermal simulation this term is determined automatically.

Results

Figures 4 and 5 show the air change rate in the summer and in the winter period respectively. The resulting air temperatures are shown in figures 6 and 7, the thermal space load factors for three periods in figure 8.

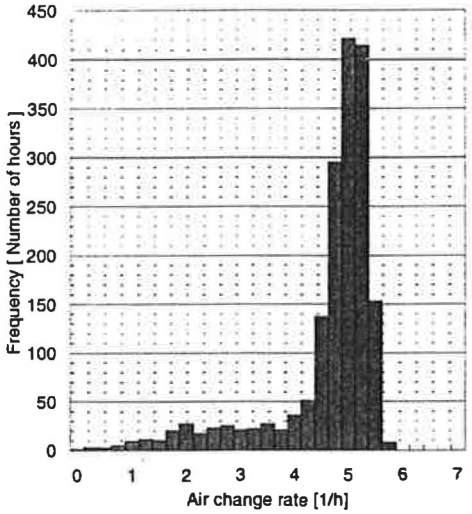

Figure 4 Air change rate during work time (7.30 - 17.30), period May - September

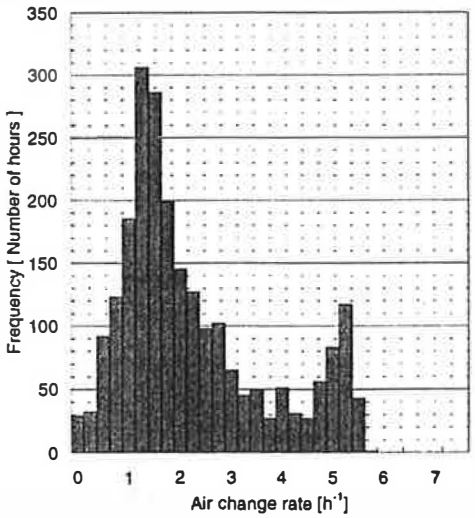

Figure 5 Air change rate during work time, period October - April

Discussion

A space load factor around 0.75 results for the important period May-September. This corresponds very well with standard values given in VDI (1997).

During the summer period high peak temperatures can be observed, which can be reduced slightly by using larger openings.

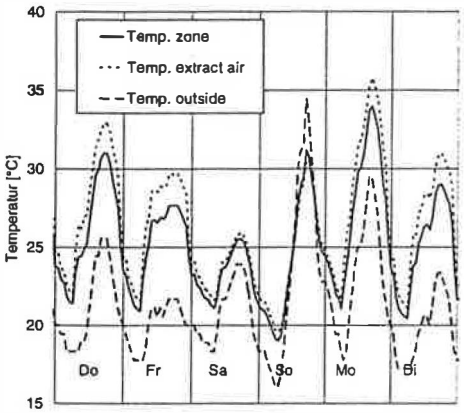

Figure 6 Temperature evolution, period 11. -16. August

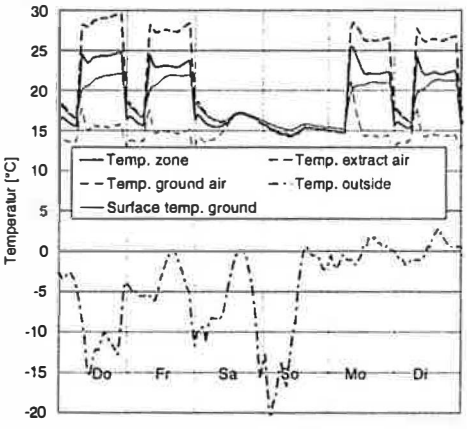

Figure 7 Temperature evolution, period 13. - 18. January

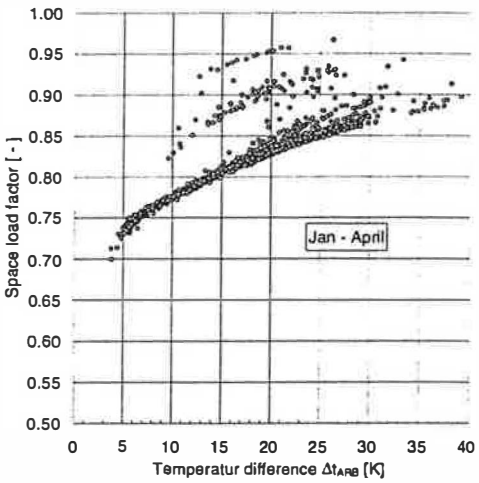

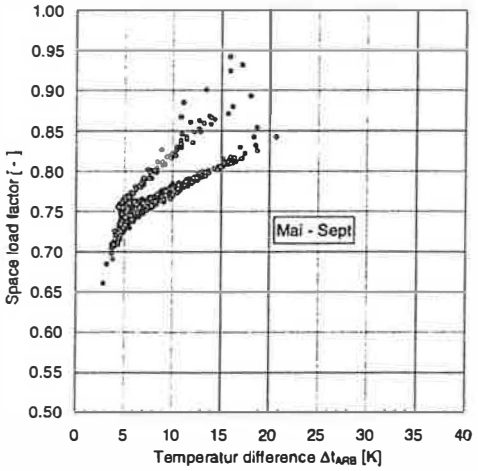

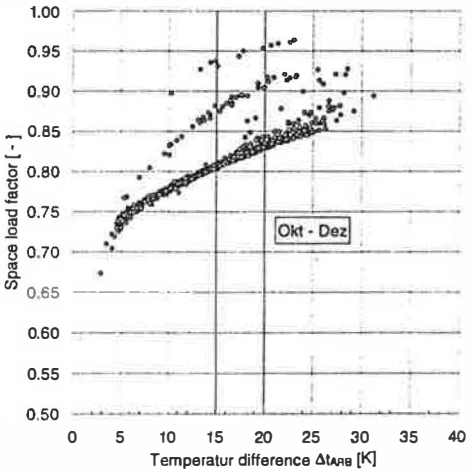

Figure 8 Space load factors μ_t during work time

FLOW THROUGH AN OPENING WITH AN INSECT SCREEN

Method

Determination of the discharge coefficient

The dynamic pressure loss by an opening is described as

$$\Delta p = \zeta \cdot \frac{\rho}{2} \cdot w^2 \tag{4}$$

or

$$w = \frac{1}{\sqrt{\zeta}} \cdot \sqrt{\frac{2 \cdot \Delta p}{\rho}} \tag{5}$$

The average speed w can be calculated from the volumetric air flow $\dot{V}$ and the effective opening area A. As the air passes through the opening it contracts to an area A which is usually smaller than the geometrical area A_g of the opening (see figure 9). The contraction coefficient C_c is the ratio of the area A to the area A_g :

$$C_c = \frac{A}{A_g} \tag{6}$$

In C_c the contraction coefficient as well as the cross section area reduction by the insect screen is included.

The air speed is

$$w = \frac{\dot{V}}{A} = \frac{\dot{V}}{C_c \cdot A_g} \tag{7}$$

With the equation (5) and (7) the volumetric air flow $\dot{V}$ is

$$\dot{V} = \frac{1}{\sqrt{\zeta}} \cdot C_c \cdot A_g \cdot \sqrt{\frac{2 \cdot \Delta p}{\rho}} \tag{8}$$

with

$$\frac{1}{\sqrt{\zeta}} = C_v \tag{9}$$

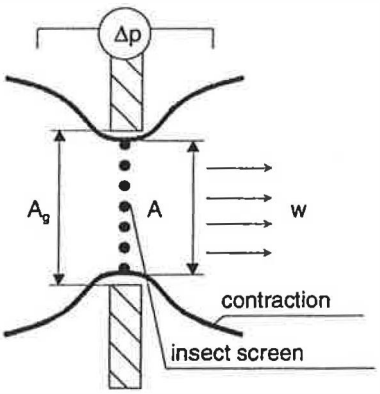

Figure 9 Schematic representation of the air flow through the lattice opening

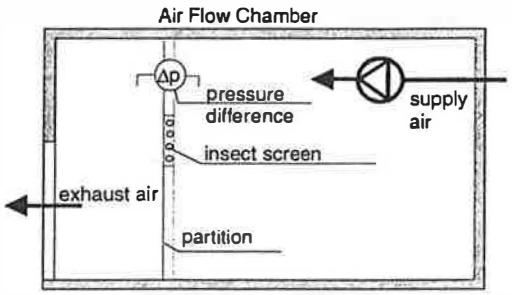

Figure 10 Schematic representation of the experimental setup in the air flow chamber

and

$$C_d = C_v \cdot C_c \tag{10}$$

resulting in

$$\dot{V} = C_d \cdot A_g \cdot \sqrt{\frac{2 \cdot \Delta p}{\rho}} \tag{11}$$

Finally the discharge coefficient C_d is

$$C_d = \frac{\dot{V}}{A_g} \cdot \sqrt{\frac{\rho}{2 \cdot \Delta p}} \tag{12}$$

In the literature, discharge coefficient values for sharp edged apertures as well as for rounded nozzles can be found. In order to check the quality of the measurement, the coefficient for an opening without insect screen was determined and compared with the literature specifications. For sharp edged apertures the literature shows that the C_d-coefficient is only slightly dependent on the air speed. This was checked by different measurements with different air speeds. A larger dependency was expected as a function of the opening's geometry.

Measurements

The air flow chamber of the EMPA was divided into two sections by a partition. The specific insect screens were successively built into this partition. The desired air flow rate was supplied with a fan and the resulting pressure difference (Δp) between the two chamber sections was measured. Based on this pressure difference (Δp), on the volumetric air flow ($\dot{V}$), the opening are A_g and on the air density ρ the C_d-coefficient was determined.

Table 1: Technical data of the examined insect screens

Grid distance [µm]	Free cross section [%]	Wire sizes [µm]
1180	59.5	350
1600	61.0	450
1800	61.0	500
4000	64.0	1000

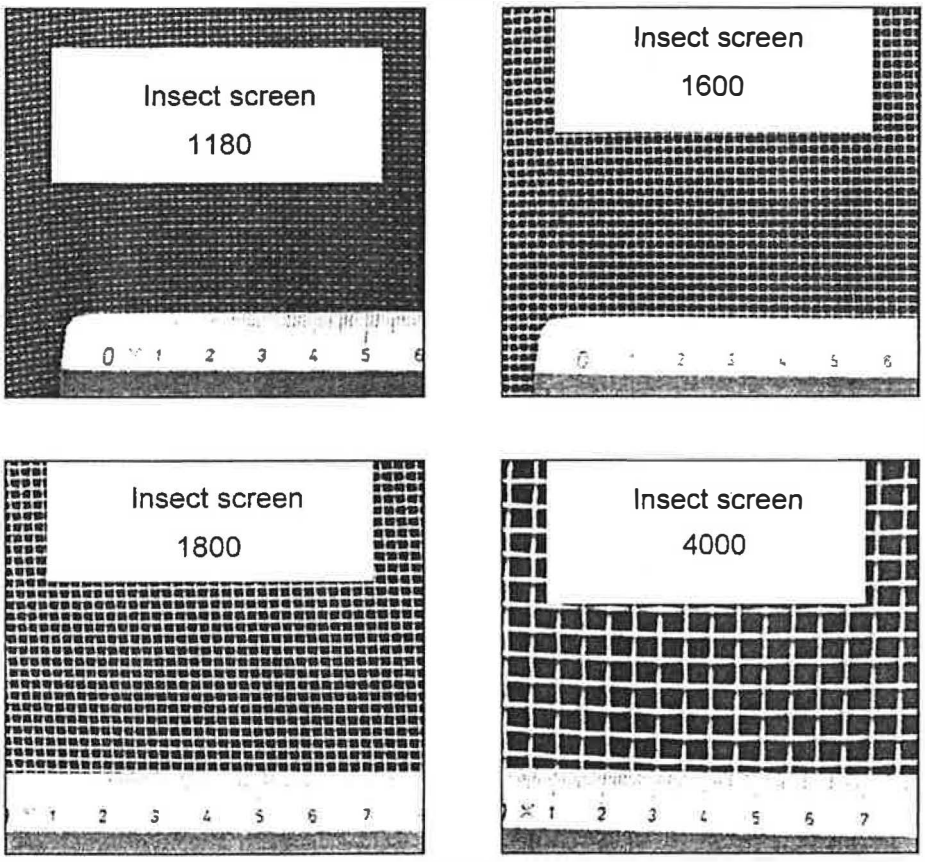

Figure 11 Pictures of the insect screens used

Results

Figure 12 shows the strong dependency of the C_d-coefficient with the hydraulic diameter and the effect of the insect screen.

For rectangular openings the hydraulic diameter can be calculated as

$$d_h = \frac{2 \cdot a \cdot b}{(a+b)} \tag{11}$$

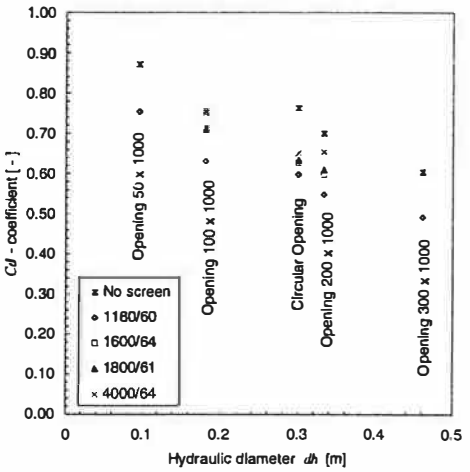

Figure 12 The C_d-coefficient in function of the hydraulic diameter.

Discussion

The additional pressure loss caused by the insect screen is low.

The C_d-coefficient of the insect screen type 1180/60 is around 0.55 according to manufacturer information. This value corresponds well with the measured values for the large, square shaped openings.

CONCLUSION

A common engineering assumption is that insect screens would decrease the air flow through an opening in proportion to the cross section reduction. The results, however, do not confirm this assumption. The discharge coefficients of the openings with insect screens are only a little smaller than the discharge coefficient of the openings without insect screen.

An explanation for this effect could be that the air flow contraction normally observed in openings without screen is reduced by the screen. In addition, the finding suggest that the hydraulic diameter has as much influence on the discharge coefficient as the type of insect screen.

The study shows that in this particular case a natural ventilation system is a suitable and ecological possibility to remove the high internal thermal loads, even with finely woven insect screens in the openings.

ACKNOWLEDGMENTS

The results presented in this paper are based on contract work for Zentralwäscherei Baset-adrett AG, Basel. Markus Koschenz and Robert Weber were responsible for this work, to whom our thanks go.

REFERENCES

AIVC (1996) *A Guide to Energy Efficient Ventilation.* The Air Infiltration and Ventilation Center, Coventry

Awbi, H. B. (1991) *Ventilation of Buildings.* E & FN SPON, London

Clima Suisse (1997) *Ventilation of Large Enclosures.* Clima Suisse, Zürich

Etheridge, D. and Sandberg, M. (1996) *Building Ventilation : Theory and Measurement.* John Whiley & Sons, Chichester

Santamouris, M. and Asimakopolous, D. (1996) *Passive Colling of Buildings.* James & James, London

VDI (1997) *Air Conditioning Systems for Factories* (in German). Beuth Verlag GmbH, Berlin

Nomenclature

Symbol	Unit	Meaning
A	m^2	Effective opening area
A_g	m^2	Geometrical opening area
A_{AB}	m^2	Discharge opening
A_{AU}	m^2	Outside air opening
a	m	Length of the opening
b	m	Width of the opening
C_c	-	Contraction coefficient
C_d	-	Discharge coefficient
C_v	-	Velocity coefficient
c_p	J/kg-K	Specific heat at constant pressure
d_h	m	Hydraulic diameter
f		Correction factor
h	m	Average room height
$\dot{m}_L$	kg/s	Supply air mass flow
n	1/h	Air change
$\dot{Q}$	W	Heat loads
$\dot{Q}_{Tot}$	W	Total thermal loads (internal and external)
$\dot{q}_{Tot}$	W/m^2	Total specific thermal loads (internal and external)
t_{AB}	°C	Exhaust air temperature
t_{ARB}	°C	Occupied zone air temperature
t_{AU}	°C	Outside air temperature
Δt_{ARB}	K	Difference between occupied zone air temperature and outside air temperature
V	m^3	Zone volume
$\dot{V}$	m^3/s	Volumetric air flow
w	m/s	Air speed
Δp	Pa	Pressure difference
μ_t	-	Space load factor
μ_g	-	Part of the total heat flow removed by air
ζ	-	Resistance coefficient
ρ	kg/m^3	Air Density